https://doi.org/10.5194/egusphere-2022-215
Preprint. Discussion started: 20 April 2022

Present and future European heat wave magnitudes: climatologies, trends, and their associated uncertainties in GCM-RCM model chains

Changgui Lin[1,2], Erik Kjellström[1,3], Renate Anna Irma Wilcke[1], and Deliang Chen[2]

[1]Rossby Centre, Swedish Meteorological and Hydrological Institute, Norrköping, Sweden
[2]Regional Climate Group, Department of Earth Sciences, University of Gothenburg, Gothenburg, Sweden
[3]Department of Meteorology and the Bolin Centre for Climate Research, Stockholm University, Stockholm, Sweden

Correspondence: Changgui Lin (mapulynn@gmail.com)

Abstract. This study investigates present and future European heat wave magnitudes, represented by the Heat Wave Magnitude Index-daily (HWMId), for regional climate models (RCMs) and their driving global climate models (GCMs) over Europe. A subset of the large EURO-CORDEX ensemble is employed to study sources of uncertainties related to choice of GCMs, RCMs and their combinations.

We initially compare the evaluation runs of the RCMs driven by ERA-interim reanalysis to the observations, finding that the RCMs are able to capture most of the observed spatial and temporal features of HWMId. With their higher resolution, RCMs can reveal spatial features of HWMId associated with small-scale processes; moreover, RCMs represent large scale features of HWMId in a satisfactory way. Our results indicate a clear added value of the RCMs in relation to their driving GCMs. Forced with the emission scenario RCP8.5, all the GCM and RCM simulations consistently project a rise in HWMId at an exponential-like rate. However, the climate change signals projected by the GCMs are generally attenuated when downscaled by the RCMs, with the spatial pattern also altered.

The uncertainty in a simulated future change of heat wave magnitudes following global warming can be attributed almost equally to the difference in model physics (as represented by different RCMs) and to the driving data associated with different GCMs. Regarding the uncertainty associated with RCM choice, representation of the orographic effects differently is a major factor. No consistent spatial pattern in the ensemble spread associated with different GCMs is observed between the RCMs, suggesting GCMs' uncertainties are transformed by RCMs in a complex manner due to the nonlinear nature of model dynamics and physics.

1 Introduction

High temperatures associated with heat waves can have adverse effects on health and have been reported to lead to excessive mortality rates among people in many regions of the world (Guo et al., 2017). In Europe, the heat waves in summer 2003 (Robine et al., 2008) and 2010 (Barriopedro et al., 2011) are prominent examples. Even in high-latitude areas, such as Scandinavia, heat waves can lead to excess mortality as reported by Åström et al. (2019) for the long and warm Swedish summer 2018

https://doi.org/10.5194/egusphere-2022-215
Preprint. Discussion started: 20 April 2022

(Wilcke et al., 2020). In addition to health problems atmospheric heat waves are often related to water shortages, increased risk of forest fires, and maritime heat waves, all of which can have severe impacts both on natural ecosystems and human society (IPCC, 2014).

The Intergovernmental Panel on Climate Change (IPCC) concluded that frequency and duration of warm spell lengths have increased in the observed past on a global scale (IPCC, 2018; Seneviratne et al., 2021). They also attribute part of the observed changes in frequency and intensity of daily temperature extremes on the global scale since the mid-20th century to increasing anthropogenic forcing of the climate system. Furthermore, projections for the future under scenarios of increasing greenhouse gas forcing indicate a continued increase in both intensity and in duration of heat waves (Molina et al., 2020). To alleviate future problems, adaptive measures are needed, even under scenarios with strong mitigation (IPCC, 2022). Climate change adaptation, in turn, requires relevant information about changes both in geographical and temporal extent as well as in intensity and duration of heat waves.

Climate model projections constitute the most prominent information about future climate that is available. International coordinated Climate Model Intercomparison Projects (CMIP), such as CMIP5 (Taylor et al., 2012) and CMIP6 (Eyring et al., 2016), provide large ensembles of global climate model (GCM) projections. GCMs, however, are most often run at coarse horizontal resolution, implying that they have a crude representation of relevant local and regional processes and often come with strong biases at the regional scale (Luo et al., 2020). As a remedy, to improve the quality of the simulated climate and add value compared to GCMs, regional climate models (RCMs) are frequently used (Torma et al., 2015; Rummukainen, 2016; Strandberg and Lind, 2021). Operated at higher resolution they more realistically represent orography, land-sea contrasts, and atmospheric processes such as mid-latitude cyclones. Large ensembles of RCM climate change projections have been produced for different continents under the auspices of CORDEX (the CoOrdinated Regional climate Downscaling EXperiment, Giorgi et al., 2009). Specifically, for Europe, joint efforts in EURO-CORDEX (Jacob et al., 2020) have resulted in more than 100 RCM projections at 0.11° grid spacing under a range of different future scenarios that are now being used for building climate services (Sørland et al., 2020; Rennie et al., 2021).

Even if RCMs add value compared to GCMs, they do not come without biases. Notably, when given input from coarse-scale GCMs that have biases in their representation of the large-scale circulation and sea-surface conditions, RCMs also show biases (e.g., Jacob et al., 2007; Vautard et al., 2020). As the RCMs often describe physical processes differently, not only biases in the historical climate, but also future climate change signals can differ from those of the underlying GCM (Coppola et al., 2021). As an example, most EURO-CORDEX RCMs have a more rudimentary treatment of aerosols and their interaction with radiative fluxes and clouds than the CMIP5 GCMs they are forced with. Consequently, discrepancies in future trends for GCM-RCM chains as reported by (Sørland et al., 2018) hace been suggested to be related to differences in aerosols and their impact on downwelling shortwave radiation (Jerez et al., 2021).

A univocal and optimal definition of heat wave can be for debate depending on impacts of interest (Perkins and Alexander, 2013; Horton et al., 2016). The Heat Wave Magnitude Index-daily (HWMId, Russo et al., 2015), a dimensionless magnitude that was designed to take into account both heat wave duration and intensity, represents an integrative approach in classifying heat waves. Indeed, it has been successfully used in a growing number of heat wave studies (e.g., Russo et al., 2016;

https://doi.org/10.5194/egusphere-2022-215
Preprint. Discussion started: 20 April 2022

Zampieri et al., 2016; Ceccherini et al., 2017; Dosio et al., 2018; Molina et al., 2020). Therefore, heat wave magnitudes are here represented by the HWMId.

The aim of this study is fourfold. First, we examine GCM-RCM combinations for Europe to investigate to what degree the RCMs can represent heat waves in the historical climate when forced by reanalysis and GCMs, respectively. Second, we investigate if there is any added value in the representation of heat waves in the RCMs compared to the driving GCMs. Third, we investigate to what extent the RCMs modify the climate change signal of HWMId compared to the GCMs. Fourth, we explore the sources of uncertainties related to choice of GCMs, RCMs, and their combinations.

2 Data and methods

2.1 Heat Wave Magnitude Index-daily (HWMId)

The HWMId is described as the maximum magnitude of heat waves occurring in a year, where a heat wave is defined as a period of at least three consecutive days with maximum temperature T above a percentile-based daily threshold for a reference period (1981–2010 herein following Russo et al. (2015), if not specified otherwise). Specifically, for a given day-of-year d (from 1 to 366), the threshold is the 90$^{\text{th}}$ percentile of the set of data A_d defined by

$$A_d = \cup_{y \in Y_{\text{ref}}} \cup_{i \in W_d^{-15,15}} T_{\text{max},y,i}, \tag{1}$$

where $\cup$ denotes the union of sets; Y_{ref} represents the years within the reference period; $W_d^{-15,15}$ is the 31-day window centered at day d; and, $T_{\text{max},y,i}$ is the daily maximum temperature of day i in year y.

For each day in an identified heat wave the daily magnitude, M_d , is calculated following:

$$M_d = \begin{cases} \dfrac{T_{\text{max},d} - T_{\text{max,ref,25p}}}{T_{\text{max,ref,75p}} - T_{\text{max,ref,25p}}} & \text{if } T_{\text{max},d} > T_{\text{max,ref,25p}} \\ 0 & \text{otherwise} \end{cases}, \tag{2}$$

where $T_{\text{max},d}$ is the daily maximum temperature of day d, and $T_{\text{max,ref,25p}}$ and $T_{\text{max,ref,75p}}$ are the 25$^{\text{th}}$ and 75$^{\text{th}}$ percentiles, respectively, of the maximum temperature time series over the reference period. M_d is calculated at each grid point. According to the definition (Eq. 2), a daily magnitude M_d equal to n indicates that the temperature anomaly of day d with respect to $T_{\text{max,ref,25p}}$ is n times the climatological interquartile range (IQR) within the reference period.

For each heat wave, the magnitude is calculated as the sum of the daily magnitudes of the constituent days is calculated. Finally, the annual maximum is identified from the individual heat waves in a year. This number is the HWMId analyzed here.

2.2 Climate model simulations and other data

The large number of GCM-RCM combinations available from EURO-CORDEX allows us to examine signals and associated uncertainties of heat wave magnitudes within the downscaling process. For that we used only a subset of the available ensemble to gain a full GCM-RCM matrix without gaps. That means, we chose three GCMs that have been downscaled by four RCMs

https://doi.org/10.5194/egusphere-2022-215
Preprint. Discussion started: 20 April 2022

Table 1. The RCMs and the driving GCMs that form the simulation matrix in the study.

Model	Institute	Resolution	Realization
RCM:			
HIRHAM5	Danish Meteorological Institute	EUR-11*	
RACMO22E	Royal Netherlands Meteorological Institute	EUR-11	
RCA4	Swedish Meteorological and Hydrological Institute	EUR-11	
REMO2015	Climate Service Center Germany	EUR-11	
GCM:			
EC-EARTH	Irish Centre for High-End Computing	T159L62	r12i1p1
HadGEM2-ES	Met Office Hadley Centre	N96L38	r1i1p1
NorESM1-M	Norwegian Climate Centre	F19L26	r1i1p1

* EURO-CORDEX rotated 0.11° (about 12.5 km) grid.

returning a 3×4 matrix of climate simulations, as listed in Table 1. The driving GCM simulations, from CMIP5, include historical runs (to 2005) forced with historical forcings and projection runs (since 2006) forced with representative concentration pathways (RCPs). Here, we only focus on RCP8.5. Three periods were defined for the calculation of the climate change signals in simulated heat wave magnitudes, termed "recent past" (1981–2020), "nearest decades" (2021–2060), and "end of the century" (2061–2100). The uncertainty across simulations is roughly described here by the spread of values (maximum − minimum) considering the limited size of the simulation matrix. The spread along the RCM dimension represents the uncertainty associated with the RCM model physics while the spread along the GCM dimension corresponds to the uncertainty associated with the driving GCM simulations.

In addition to the GCM-RCM combinations that compose the matrix, the EURO-CORDEX initiative also provides a set of evaluation runs, for which the participating RCMs are forced with boundary conditions from the ERA-Interim reanalysis (Dee et al., 2011). This type of simulation, which is often referred to as perfect-boundary conditions run, allows for an in-depth comparison with the observed climate including also its temporal evolution. In the first part of the study, we compared these evaluation runs to observations, as well as the ERA-Interim reanalysis data. The observational data used in the study are from the E-OBS daily gridded data set version 20.0e of the European Climate Assessment & Data (Cornes et al., 2018, ECA&D, www.ecad.eu), which covers Europe at a 0.1° regular grid spacing for the period from 1950 to July 2019. Of note, the years 1989–2008 were deployed as both the reference period for calculating HWMId and the analysis period in the comparison, since it is the shared period covered by all the RCMs' evaluation runs.

Mean bias error (MBE), root mean square error (RMSE), and Pearson correlation coefficient (r) were adopted as performance indicators for a model in simulating HWMId compared to E-OBS. They quantify the degree of an overall overestimation/underestimation, the degree of closeness in values, and the association in variations, respectively. When these indicators were applied for spatial patterns, they were calculated after the simulation data were remapped to the ERA-Interim grids. The

https://doi.org/10.5194/egusphere-2022-215
Preprint. Discussion started: 20 April 2022

remapping was done conservatively for each model. RMSE and r were also used to determine the similarity in spatial pattern between simulations.

To further explore the underlying processes of the simulated climate change signals of HWMId, the simulated climate change signals in annual mean $T_{\max}$, dry days (with precipitation < 1 mm), and effective precipitation (precipitation $-$ evaporation) were investigated.

3 Results

3.1 Evaluation of reanalysis-driven RCMs in simulating historical heat waves

Among various aspects of heat waves, we want to answer the following questions: i) if the spatial pattern of the climatological mean reveals observed local information, and ii) if the regional mean shows the same signal/response of large-scale climate variations as observations.

Figure 1a shows the comparison of the spatial pattern of the climatological mean of HWMId over 1989–2008 for the evaluation runs of the RCM considered. Observations (E-OBS) indicate a clear west-east gradient, with HWMId values in western coastal areas on average 1.2 higher than those in eastern areas. The same pattern is confirmed by reanalysis data (ERA-Interim), which is used as boundary and initial conditions for the evaluation RCM simulations. The RCM evaluation runs can reproduce the observed west-east gradient. Though all RCM simulations agree on the general spatial pattern, they do differ in representing details of some local features. As the RCMs were driven by the same reanalysis, the differences among the RCM simulations should be related to differences in model physics which may be an important source of uncertainty in simulating extreme heat waves. Ignoring the spatial pattern and only focusing only on the percentage of the land area exceeding certain HWMId values (Fig. 1b), we find a close agreement between the RCM simulations, although a slight overestimation was found at the high end tail of the HWMId distribution (HWMId$\geq$9 or 10). The overestimation for RACMO22E is apparent for most of HWMId values (7 to 10).

Averaged in space, the RCM evaluation runs reproduce generally, but not perfectly, the temporal evolution of the observed HWMId as shown by the heat-map in Fig. 2a. Years with high HWMId values (1994, 2003, 2006, and 2007) are captured by all the RCMs. However, the RCMs fail in reproducing the ranking of these years by occasionally overestimating or underestimating the HWMId values. For example, RACMO22E overestimates HWMId excessively in 1995 as does RCA4 in 1997. Moreover, some RCM simulations show an overestimation of HWMId compared to the observations. Reflecting on the distribution function as shown in Fig. 2b, the HWMId values simulated by the RCMs show an overestimation of the 75$^{\text{th}}$ percentile and the median, while deviations for the 25$^{\text{th}}$ percentile are smaller with REMO2015 showing an underestimation and HIRHAM5 and RACMO22E overestimations (Fig. 2b). Both HIRHAM5 and the multi-RCM mean show a better representation of the observed IQR but shifted to higher values and, in addition, with a shorter right tail, which means too weak heat wave extremes. At the same time, and in contrast to E-OBS and ERA-Interim, all the RCMs have individual years with HWMId values lower than the observations, indicating that there are also underestimations of heat waves.

https://doi.org/10.5194/egusphere-2022-215
Preprint. Discussion started: 20 April 2022

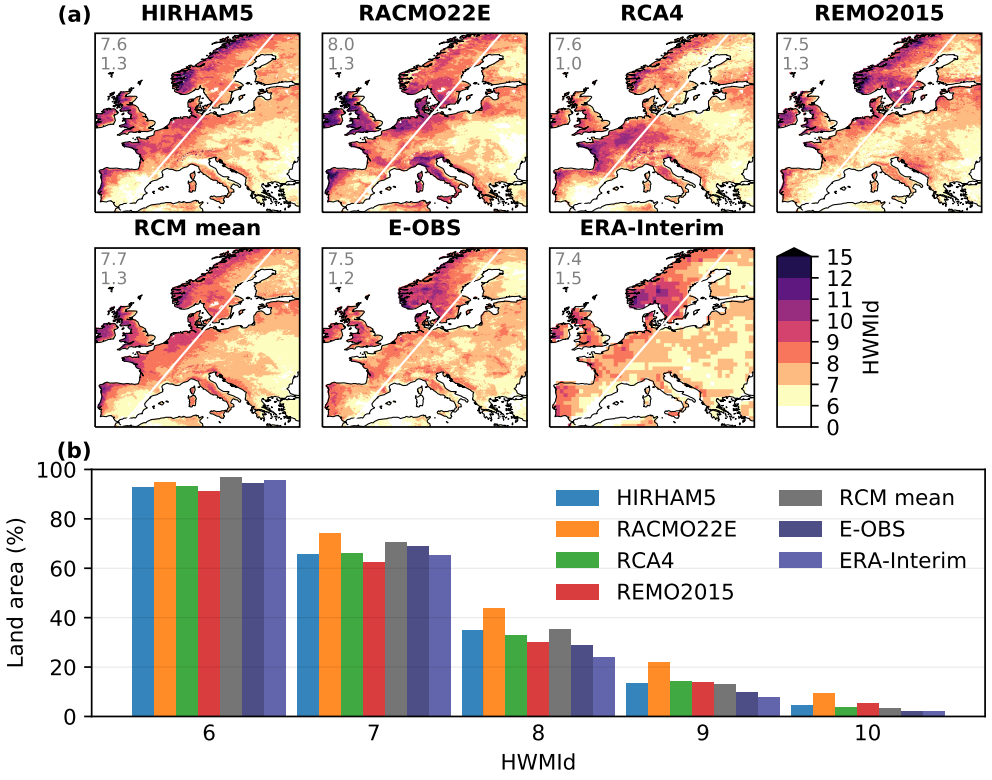

Figure 1. Climatological mean HWMId over 1989–2008 in the four RCMs' evaluation runs, the multi-RCM mean, E-OBS, and ERA-Interim: (a) spatial pattern, and (b) percentage of the land area exceeding certain HWMId levels (HWMId≥6, 7, 8, 9, or 10). The two numerals in each map shows the area-weighted average over the entire domain and the difference between western and eastern parts divided by the white line, respectively.

According to RMSE and r, REMO2015 has the best performance among the selected four RCMs in representing the spatial pattern of the climatological mean HWMId (Table 2) whereas HIRHAM5 outperforms the other RCMs in reproducing the temporal evolution of the regional mean (Table 3). For both spatial and temporal measures, the multi-RCM mean has generally smaller RMSE and higher r than most of the individual RCMs, probably due to a compensation of deficiencies of each RCM in representing different processes. We also note that all RCMs show less agreement with E-OBS in RMSE and r compared to that of ERA-Interim.

3.2 Evaluation of heat waves in GCM-driven RCMs under the recent past climate

A similar comparison as for the ERA-Interim-driven runs discussed above was conducted for the GCM-driven runs as well as for the driving GCM simulations. We present the MBE, RMSE, and r (of spatial measures) against E-OBS for the climatological mean HWMId under the evaluation period (1989–2008) in Table 4. Comparing Table 4 with Table 2, we can investigate the influence of the shift of driving data from the ERA-interim reanalysis to GCM simulations. Next, the climatological mean

https://doi.org/10.5194/egusphere-2022-215
Preprint. Discussion started: 20 April 2022

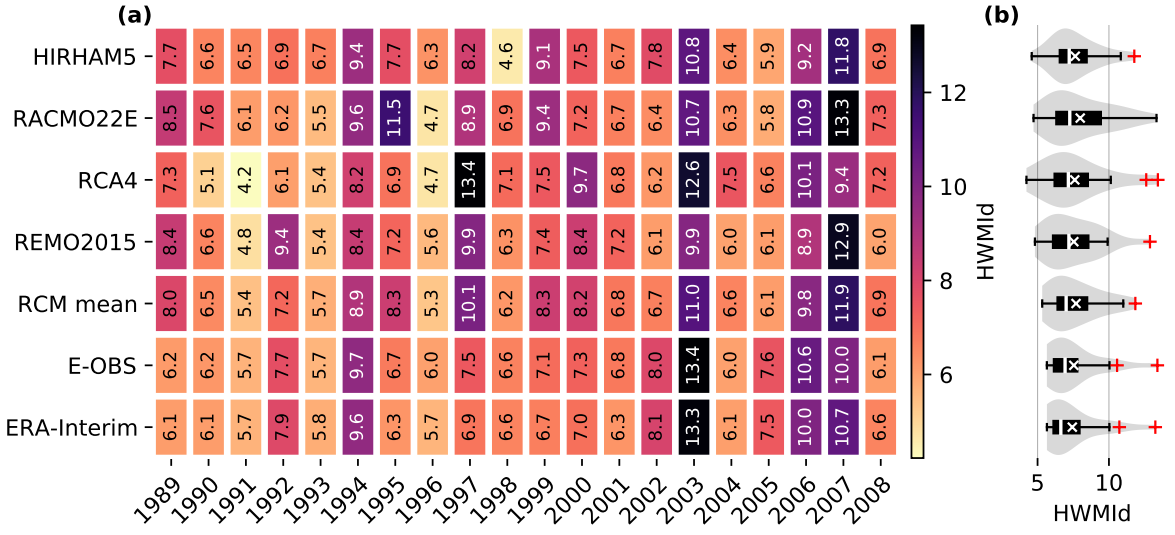

Figure 2. Regional mean HWMId from 1989 to 2008 in the four RCMs' evaluation runs, the multi-RCM mean, E-OBS, and ERA-Interim: (a) temporal evolution, and (b) corresponding violin/box plot. The violin plots (light-gray areas) represent the data distribution based on a Gaussian kernel density estimation using Scott's rule. In each box plot, the box limits represent lower and upper quartiles; the white line and 'x' marker inside the box are the median and the mean, respectively; and the outliers marked with red plus signs outside of the whisker lie at least 1.5 times the IQR away from the box limits.

Table 2. MBE, RMSE, and r of spatial measures for the climatological mean HWMId over 1989–2008 in ERA-Interim, the four RCMs' evaluation runs, and the multi-RCM mean, with E-OBS as reference.

	ERA-Interim	HIRHAM5	RACMO22E	RCA4	REMO2015	RCM mean
MBE	−0.13	0.12	0.45	0.08	0.00	0.17
RMSE	0.55	0.89	1.17	1.03	0.76	0.74
r^*	0.86	0.70	0.60	0.53	0.79	0.77

* All are statistically significant at $p < 0.01$.

HWMId under the recent past climate (1981–2020) was investigated, with the spatial pattern shown in Fig. 3 and the MBE, RMSE, and r (of spatial measures) presented in Table 5.

Comparing Table 4 with Table 2 shows that the GCMs perform poorly in simulating spatial characteristics of HWMId compared with ERA-Interim (RMSE: 1.02–1.26 vs. 0.55, and r: 0.17–0.43 vs. 0.86), whereas GCM-driven RCM simulations show similar results as the ERA-Interim-driven ones, which becomes in particular obvious for RMSE (0.97–1.37 vs. 0.76–1.17). This implies an improvement in the representation of the spatial characteristics of HWMId introduced by the downscaling with RCMs.

https://doi.org/10.5194/egusphere-2022-215
Preprint. Discussion started: 20 April 2022

Table 3. Similar to Table 2 but of temporal measures for the time series of regional mean HWMId from 1989–2008.

	ERA-Interim	HIRHAM5	RACMO22E	RCA4	REMO2015	RCM mean
MBE	−0.11	0.10	0.45	0.07	−0.00	0.16
RMSE	0.35	1.22	1.84	1.75	1.53	1.25
r^*	0.99	0.78	0.64	0.68	0.68	0.78

* All are statistically significant at $p < 0.01$.

Table 4. Similar to Table 2 but for the selected GCM simulations and the GCM-driven simulations that compose the RCM simulation matrix (columns for RCMs and rows for their driving GCMs). It is worth noting that the statistics were calculated for the climatological mean HWMId over the evaluation period (1989–2008), where the HWMId has the reference period also being 1989–2008, the same as those in Table 2. For each statistic, an additional row is given for the column mean (i.e., along the GCM dimension) of the driving GCM simulations and the RCM simulation matrix.

	GCM	HIRHAM5	RACMO22E	RCA4	REMO2015	RCM mean
MBE:						
EC-EARTH	−0.21	−0.09	0.19	0.17	−0.21	0.02
HadGEM2-ES	0.17	0.13	0.86	0.36	−0.40	0.25
NorESM1-M	0.49	0.08	0.36	0.54	−0.06	0.24
Model mean	0.02	0.04	0.47	0.37	−0.22	
RMSE:						
EC-EARTH	1.15	1.01	1.12	1.31	1.07	0.94
HadGEM2-ES	1.02	0.97	1.35	1.26	0.97	0.88
NorESM1-M	1.26	1.05	1.37	1.34	1.03	0.98
Model mean	0.95	0.85	1.08	1.10	0.87	
r^*:						
EC-EARTH	0.17	0.51	0.43	0.27	0.45	0.50
HadGEM2-ES	0.43	0.62	0.40	0.34	0.62	0.59
NorESM1-M	0.42	0.48	0.30	0.13	0.47	0.46
Model mean	0.36	0.61	0.45	0.33	0.60	

* All are statistically significant at $p < 0.01$.

As expected, due to the relatively large overlap in time, the observed spatial distribution under the recent past climate, as revealed by E-OBS (Fig. 3), is similar to that in the evaluation period (Fig. 1); but the shift in time (for both the reference period as the basis of HWMId and the period over which the data were analyzed) has led to an increase from on average about

https://doi.org/10.5194/egusphere-2022-215
Preprint. Discussion started: 20 April 2022

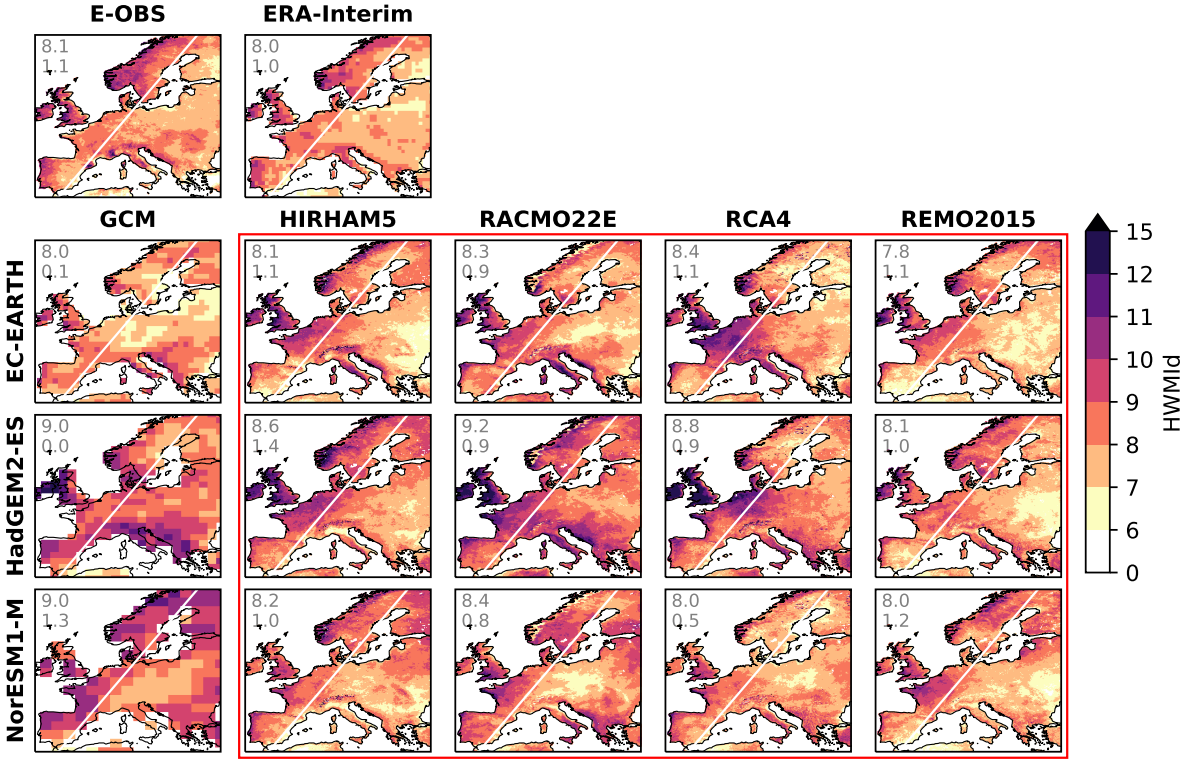

Figure 3. Climatological mean HWMId under the recent past climate (1981–2020) in the RCM simulation matrix (inside the red rectangle; columns for RCMs and rows for their driving GCMs) as well as the driving GCM simulations. Data from E-OBS and ERA-Interim are also shown for comparison. The two numerals in each map show the area-weighted average over the entire domain and the difference between western and eastern parts divided by the white line, respectively.

7.5 to about 8.0 on a continental basis with an increase mainly in Mediterranean parts of Europe. The GCMs capture some of the observed spatial pattern but miss out both in detailed structure and amplitude (Fig. 3). The observed west-east gradient is hardly seen in the GCM simulations: EC-EARTH and HadGEM2-ES report no difference between the western and eastern parts (divided by the white line on the map), while NorESM1-M shows a west-east gradient of 1.3, which is even higher than for E-OBS but simulates excessively high HWMId values in the easternmost part of the domain. In general, the downscaling with RCMs improves the representation of the observed spatial pattern (other than a few cases of RACMO22E and RCA4) and they show smaller RMSE and higher r compared to their driving GCMs (Table 5). Similar to the case of the evaluation runs (Table 2), the multi-RCM (row) means driven by a GCM simulation show a better performance compared to most of the individual RCMs. The case is also true for the GCM dimension; i.e., for each RCM, the ensemble mean across the three driving GCMs outperforms an individual ensemble member.

Furthermore, there is no accordance on which GCM that performs best among the three in reproducing the observed spatial pattern of HWMId when considering different performance indicators; e.g., EC-EARTH has the smallest MBE/RMSE whereas

https://doi.org/10.5194/egusphere-2022-215
Preprint. Discussion started: 20 April 2022

Table 5. Similar to Table 4 but for the recent past (1981–2020, with the reference period of 1981–2010).

	GCM	HIRHAM5	RACMO22E	RCA4	REMO2015	RCM mean
MBE:						
EC-EARTH	−0.14	0.03	0.19	0.26	−0.31	0.05
HadGEM2-ES	0.91	0.47	1.07	0.71	−0.31	0.55
NorESM1-M	0.95	0.06	0.31	−0.08	−0.15	0.04
Model mean	0.40	0.18	0.52	0.30	−0.17	
RMSE:						
EC-EARTH	1.05	1.03	1.07	1.19	1.02	0.91
HadGEM2-ES	1.40	1.15	1.48	1.46	0.97	1.09
NorESM1-M	1.51	1.00	1.24	1.08	1.08	0.95
Model mean	1.05	0.93	1.09	1.06	0.92	
r*:						
EC-EARTH	0.37	0.61	0.51	0.50	0.59	0.62
HadGEM2-ES	0.45	0.57	0.55	0.38	0.59	0.59
NorESM1-M	0.35	0.48	0.27	0.34	0.44	0.48
Model mean	0.42	0.61	0.52	0.47	0.60	

* All are statistically significant at $p < 0.01$.

HadGEM2-ES has slightly higher r (Table 5). The RCMs, however, do not follow the same error pattern as their driving GCMs. We also observed a large spread in the regional average across the GCMs, which is reduced by all RCMs. Moreover, in spite of the large difference in the spatial pattern of HWMId between the three GCMs, the simulations for each RCM driven by the three GCMs behave very similar to each other, as reflected by the lower RMSE and higher r between the RCM simulations compared to those between the driving GCMs (Table S1). Likewise, when driven by one GCM, the simulations of different RCMs also most often tend to be more similar to each other than to the driving GCM (i.e., higher RMSE and lower r within the "GCM" column compared to other columns in Table S2). Thus, it is interesting to explore the influences of driving data versus model physics on the uncertainty for the RCMs in simulating heat wave magnitudes under the recent past climate.

Along the RCM dimension of the matrix (i.e., RCMs with a same driving GCM), the ensemble spread of HWMId values is on average close to one fifth of the ensemble mean on a continental basis (Fig. 4). A slightly lower spread/mean ratio is observed along the GCM dimension (Fig. 5), indicating that the uncertainties associated with driving data are in similar magnitude as those associated with model physics. However, different features can be observed in the spatial pattern of ensemble spread along the two dimensions. As presented in Fig. 4, the ensemble spread along the RCM dimension shows high values mostly in mountainous areas such as the Scandinavian Mountains and the Alps, suggesting the disagreement in the orographic effects

https://doi.org/10.5194/egusphere-2022-215
Preprint. Discussion started: 20 April 2022

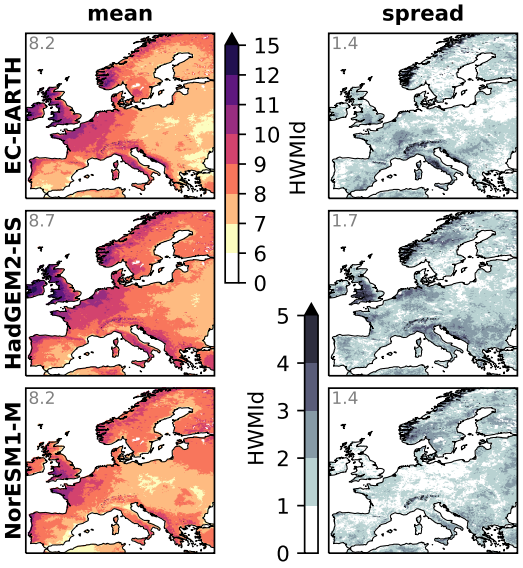

Figure 4. Ensemble mean and spread (maximum − minimum) of simulated HWMId under the recent past climate (1981–2020) for each row in the RCM simulation matrix indicating the uncertainty associated with different RCMs. The numeral in each map shows the area-weighted average.

on heat wave magnitudes across the RCMs as one of the major sources of the uncertainty associated with model physics. Aggregating the RCM matrix as well as their driving GCM simulations on the GCM dimension, meaning calculating the mean and the spread for each RCM with different GCMs, shows a similar pattern to the ensemble mean (first row of Fig. 5) but exists considerable differences in the spread (second row Fig. 5) of the RCM ensembles. A quantitative analysis regarding the similarity based on RMSE and r is presented in Table S3. Higher degree of correlation between RCMs than between any RCM and the GCMs, in combination with lower RMSE (in all but one), indicate that the RCMs tend to produce more similar results both in terms of the ensemble mean and spread. This observation implies that the uncertainties of GCMs in simulating heat wave magnitudes would not be simply inherited by RCMs but are transformed in a nonlinear manner due to the complex model dynamics and physics.

3.3 Simulated future change in heat wave magnitudes

Change in the climatological mean HWMId relative to the recent past climate was investigated for two future periods within the century: the nearest decades (2021–2060) and the end of the century (2061–2100). Figure 6 presents the spatial pattern in each of the simulations. For the two periods, apart from a strong increase in HWMId in the end of the century (approximately three times or more of that in the nearest decades), no notable difference is observed in the spatial pattern according to the spatial r. Similar to the results of the recent past climate (Sect. 3.2), a large spread of HWMId increase is seen across the GCMs. The RCMs narrow the spread, reflected by the fact that they deliver relatively moderate signals of change compared to the driving

https://doi.org/10.5194/egusphere-2022-215
Preprint. Discussion started: 20 April 2022

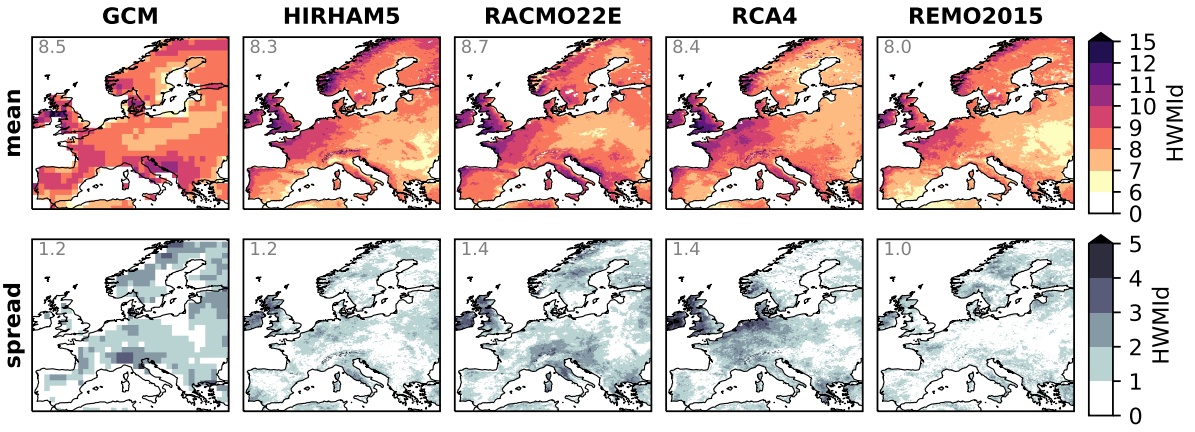

Figure 5. As Fig. 4 but for the columns of the RCM simulation matrix indicating the uncertainty associated with driving data (boundary and initial conditions). Ensemble mean and spread of the driving GCM simulations are also presented for comparison.

HadGEM2-ES and NorESM1-M. The spatial pattern of HWMId changes among the RCM simulations is similar both along the RCM dimension and the GCM dimension: indicating a stronger rise in northern and southern Europe whereas comparatively moderate for the central domain. This partly differs from the GCM simulations, which tend to show a more pronounced south-north gradient in the increase in HWMId, and also differs from the climatological mean HWMId under the recent past climate, which displays a generally west-east gradient (Fig. 1). The ensemble spread, along either the RCM dimension (Fig. 7) or the GCM dimension (Fig. 8), has a magnitude most often exceeding half of the ensemble mean on a continental basis and to some extent follows the spatial distribution of the ensemble mean (with spatial r from 0.50 to 0.92; not shown). This suggests that the driving GCM-data and the RCMs contribute about equally to the uncertainty in simulating climate change in heat wave magnitudes. For the ensemble spread, however, high values in mountainous areas are more common along the RCM dimension than along the GCM dimension. This underlines again that processes related to orography are a major source of uncertainty related to future changes in heat wave magnitudes in Europe.

The percentages of the land area exceeding certain HWMId levels (Fig. 9) provide us with a special form of survival function (complementary cumulative distribution function) to investigate probability distribution of climatological mean HWMId values across the domain regardless of geophysical location. All model simulations can reproduce the observed data probability distribution of HWMId values (solid lines) within ± 15 %. A considerable rise in the future is projected by all the simulations. In the end of the century (2061–2100), the entire domain is projected to be with HWMId values higher than the highest that has been experienced until now. The rise is across the whole probability range at an exponential rate and even more severe for the tail of HWMId distribution. As indicated in Fig. 6 the RCMs show a tendency to smoothen the change signal in the driving GCM simulations, particularly when driven by HadGEM2-ES and NorESM1-M. The only exception is RCA4 downscaling EC-EARTH. Again, we note that the RCMs generally are more alike than their driving GCMs, though RCA4 shows a pattern

https://doi.org/10.5194/egusphere-2022-215
Preprint. Discussion started: 20 April 2022

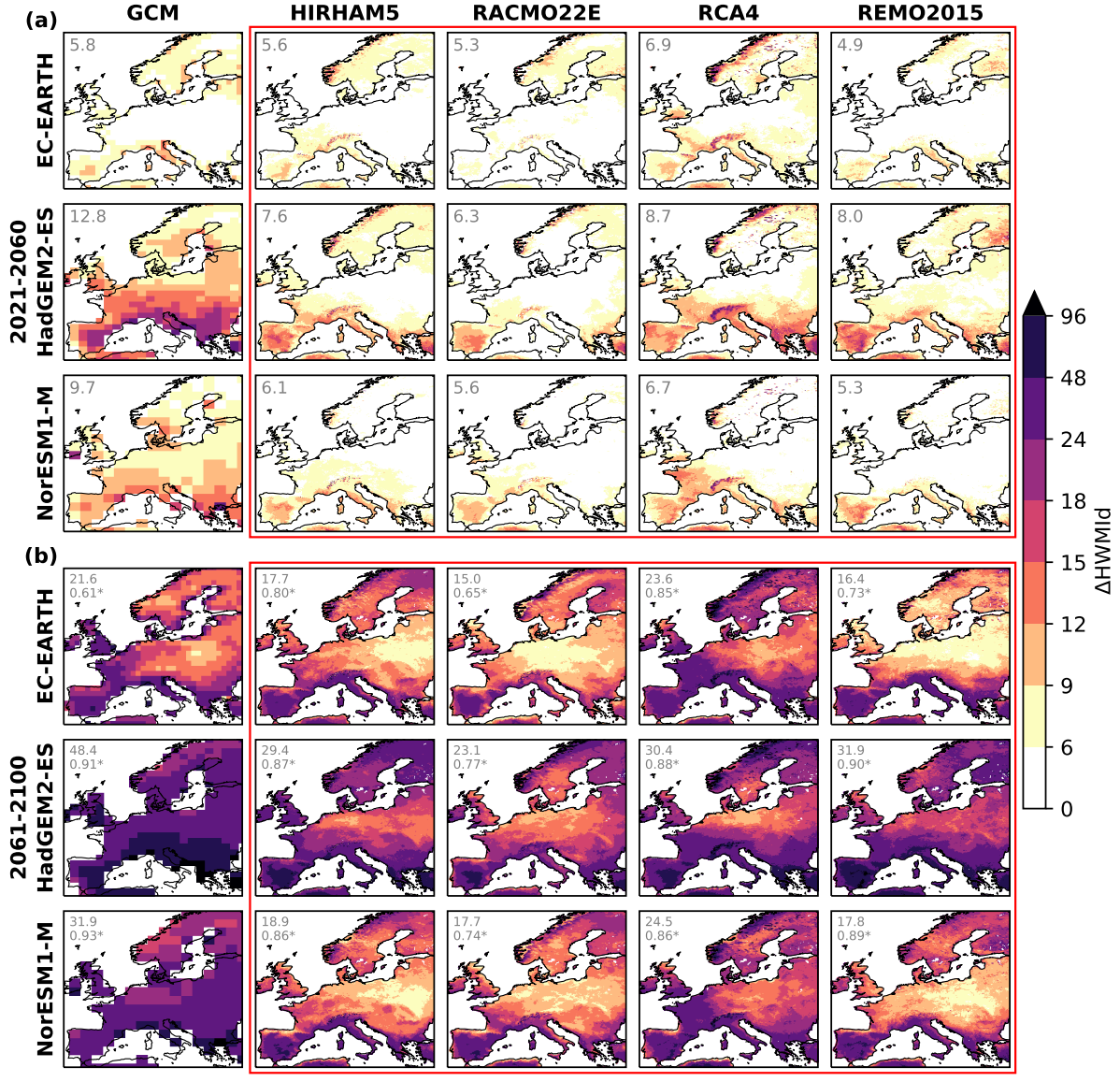

Figure 6. Change in climatological mean HWMId in the nearest decades (a: 2021–2060) and in the end of the century (b: 2061–2100) relative to the recent past climate (Fig. 3). The first numeral in each map shows the area-weighted average, and the second (only presented in b) is the spatial r between the two periods (with '*' indicating statistically significant at $p < 0.05$)

closest to the GCMs. Finally, we note that the spread between the simulations, and hence the uncertainty, increase strongly over time.

Probability distributions are also investigated for the region-wide annual HWMId values in the defined three periods, as shown in Fig. 10. As revealed by E-OBS and ERA-Interim, the region-wide HWMId for the recent past climate is represented

https://doi.org/10.5194/egusphere-2022-215
Preprint. Discussion started: 20 April 2022

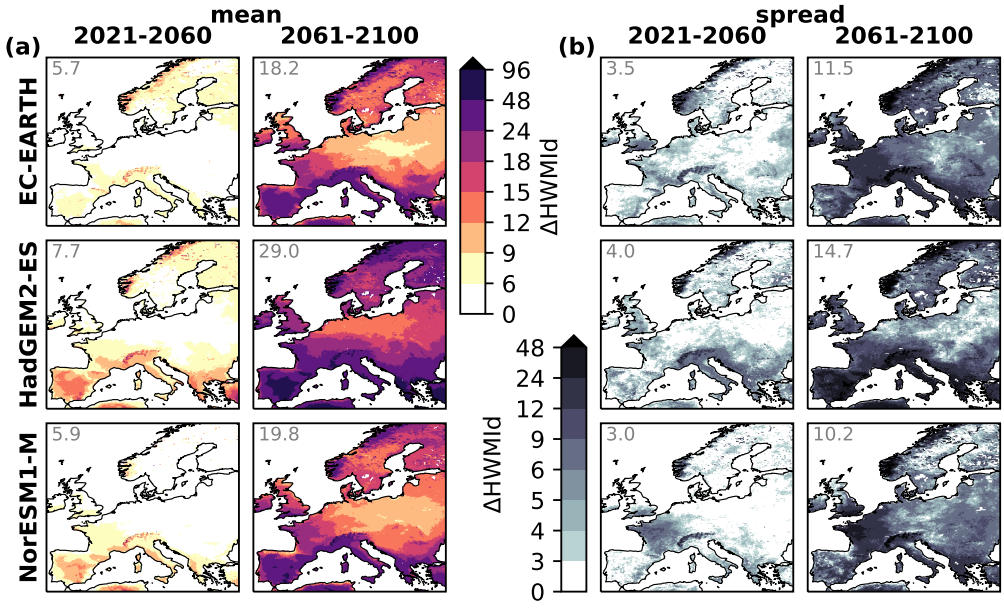

Figure 7. As Fig. 4 but for the climate change in HWMId.

by a positively-skewed distribution, or rather a quasi-log-normal distribution (as demonstrated by the quasi-normal shape of the violin plot in Fig. 10b with a logarithmic-scale x-axis). As discussed for the ERA-Interim driven simulations (Fig. 2), also the GCM-driven RCMs can to some extent capture the shape of the distribution as well as the median, but with a wider value-range for each simulation. Most of the simulations keep the shape of distribution as the values increase in the future (especially for the nearest decades), whereas some (e.g., HadGEM2-ES, RCA4 driven by EC-EARTH, and RACMO22E driven by NorESM1-M) display a distribution even with a negative skewness for the end of the century (mostly visible with logarithmic axis presented in Fig. 10b), which indicates that high HWMId values become more common. In addition to increasing levels of HWMId, also the spread defined by the ranges increase in the future. With a logarithmic-scale x-axis, we observe interesting features in the change signal: i) The mean and the median increase approximately at a constant exponential rate; ii) the width of logarithmically-transformed distribution does not change much from one period to another, i.e., a rise approximately at a constant exponential rate for both the low and high ends of HMWId values.

4 Discussion

4.1 Added value of RCMs compared to GCMs

With more small-scale processes being resolved, added value is expected from dynamical downscaling with an RCM compared to its driving GCM on the regional scale. Indeed, a large number of previous studies (e.g., Torma et al., 2015; Rummukainen, 2016; Strandberg and Lind, 2021) have reported such added value by RCMs in many respects. Thus, it is of great interest if

https://doi.org/10.5194/egusphere-2022-215
Preprint. Discussion started: 20 April 2022

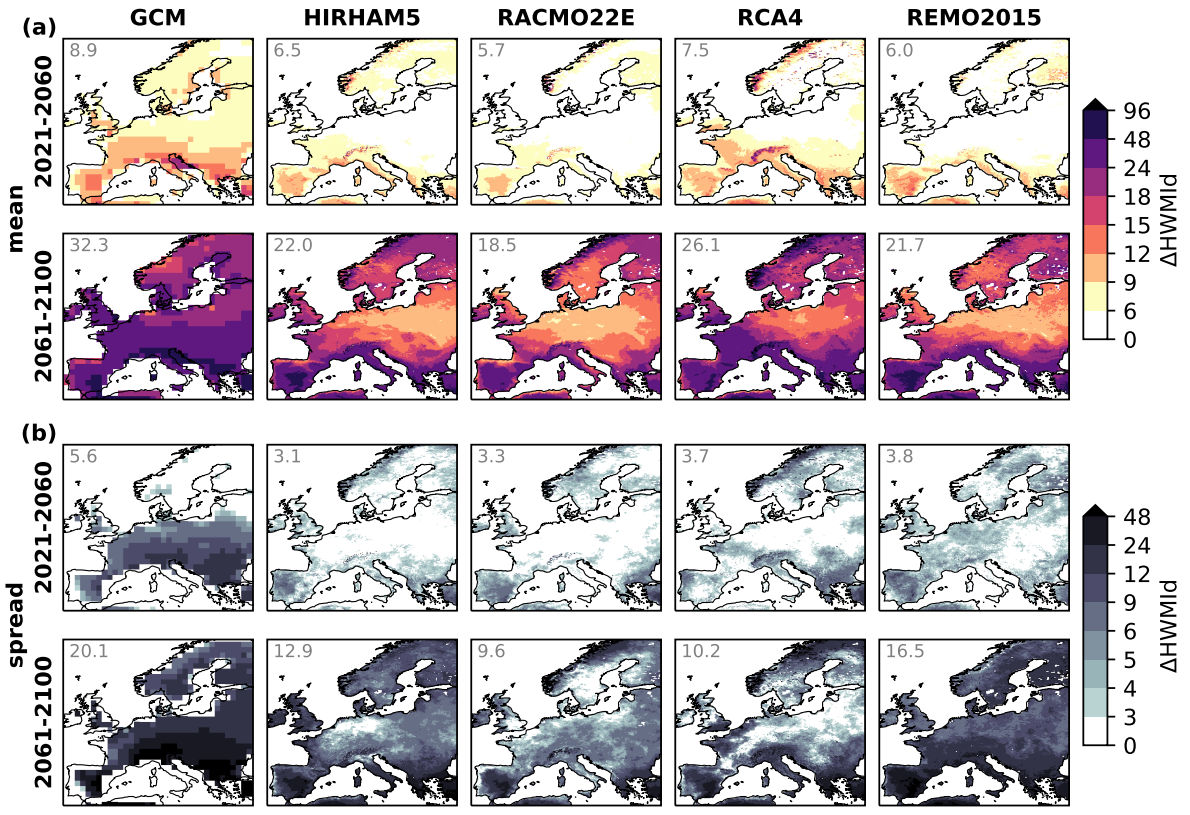

Figure 8. As Fig. 5 but for the climate change in HWMId.

RCMs create added value also for heat wave magnitudes. Compared to variables directly simulated in a climate model such as temperature and precipitation, a model with even better performance may be required to realistically represent an index with a complicated definition like HWMId; i.e., the model must be able to capture not only the mean magnitude but also the intra-annual temporal evolution of daily maximum temperature in order to realistically represent HWMId. Before discussing any potential added value we assess the degree to which the studied RCMs can represent the observed HWMId under the historical climate when driven by reanalysis data (i.e., perfect boundary conditions). We showed in Sect. 3.1 that the ERA-interim-driven runs generally reproduce the spatial and temporal patterns of the observed annual heat wave magnitudes over Europe. However, the RCMs clearly add their own signature to the results leading to a larger variability in the spatial distribution of HWMId than reflected in E-OBS and ERA-Interim (Fig. 1). It would need a more in-depth event-based analysis to see which events are large-scale triggered from the boundaries of the RCMs and thereby picked up by the RCMs, and which events are triggered inside the RCM domain and therefore possibly missed or reproduced differently by the different RCMs. One example for a large-scale-driven event could be the year 2003, where the HWMId is picked up clearly by all the RCMs in its high intensity (Fig. 2).

https://doi.org/10.5194/egusphere-2022-215
Preprint. Discussion started: 20 April 2022

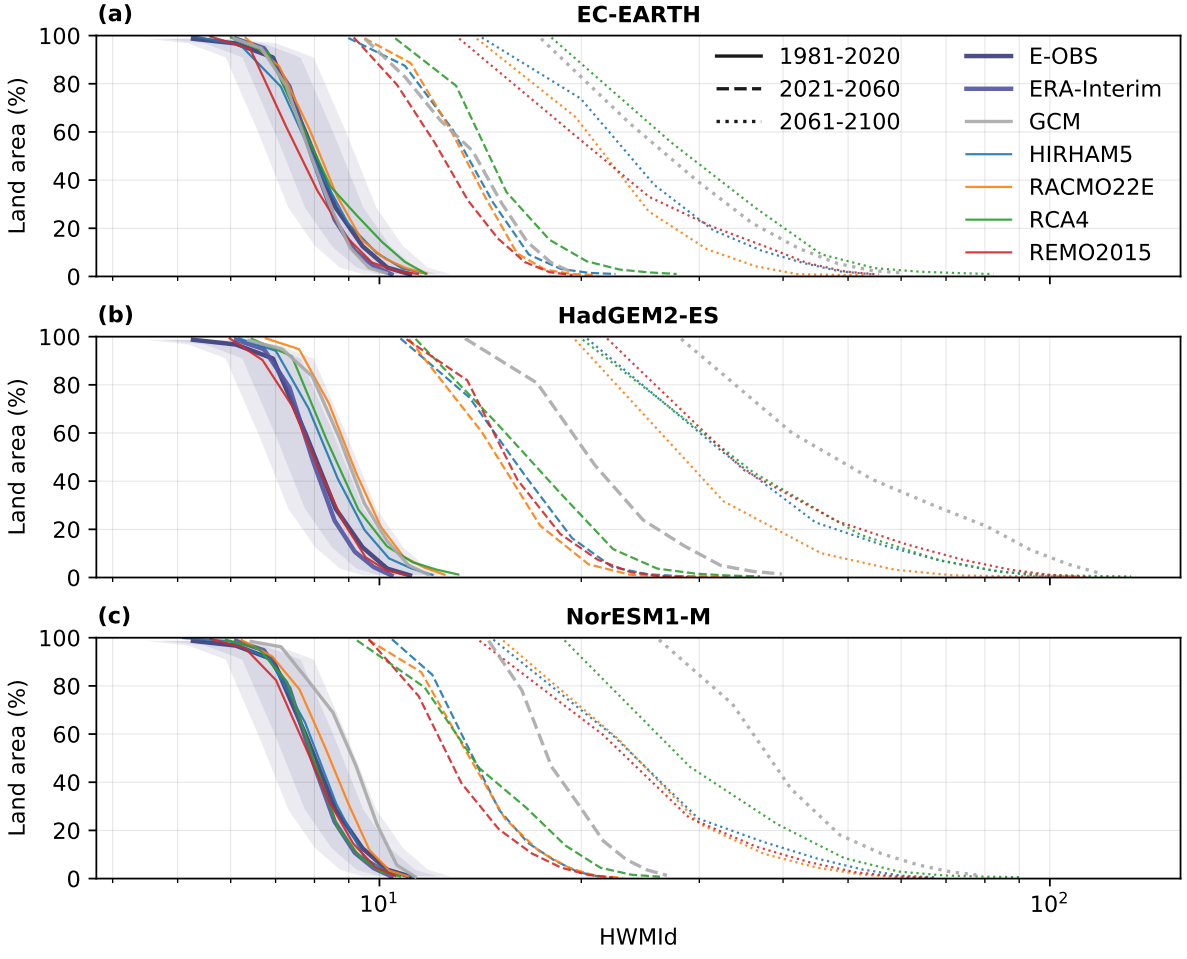

Figure 9. Percentage of the land area exceeding certain HWMId levels during the defined three periods (identified by the line styles), grouped by the driving GCMs: (a) EC-EARTH, (b) HadGEM2-ES, and (**c**) NorESM1-M. Colors represent different RCMs and gray the GCMs themselves. Data from E-OBS and ERA-Interim are also shown for comparison under the recent past climate. The shaded areas indicate within ±10 % (relatively dark) and ±15 % (light) of E-OBS data. Note that a logarithmic-scale x-axis is used.

255 The three GCM simulations accounted for, roughly reproduce the observed patterns for the recent past climate, but miss out on details in structure and amplitude (Fig. 3). The RCMs downscaling these GCMs do well in adding more detailed geographical patterns and, furthermore, pull the results closer to the observations. Again, the RCMs add their own pattern, e.g., the lower HWMId values over Eastern Europe in REMO2015. Signatures of the RCMs can also be demonstrated by the high similarity in HWMId spatial pattern between the simulations for each RCM despite a large difference between the 260 driving GCMs (Table S1). The RCMs also inherit signals from their driving GCMs. This is clearer for RACMO22E among the four RCMs, as the simulations with RCAMO22E show the highest r (except when driven by NorESM1-M) and the lowest RMSE against its driving GCMs (Table S2). Despite the inherited signals from their driving GCMs, the simulations of different

https://doi.org/10.5194/egusphere-2022-215
Preprint. Discussion started: 20 April 2022

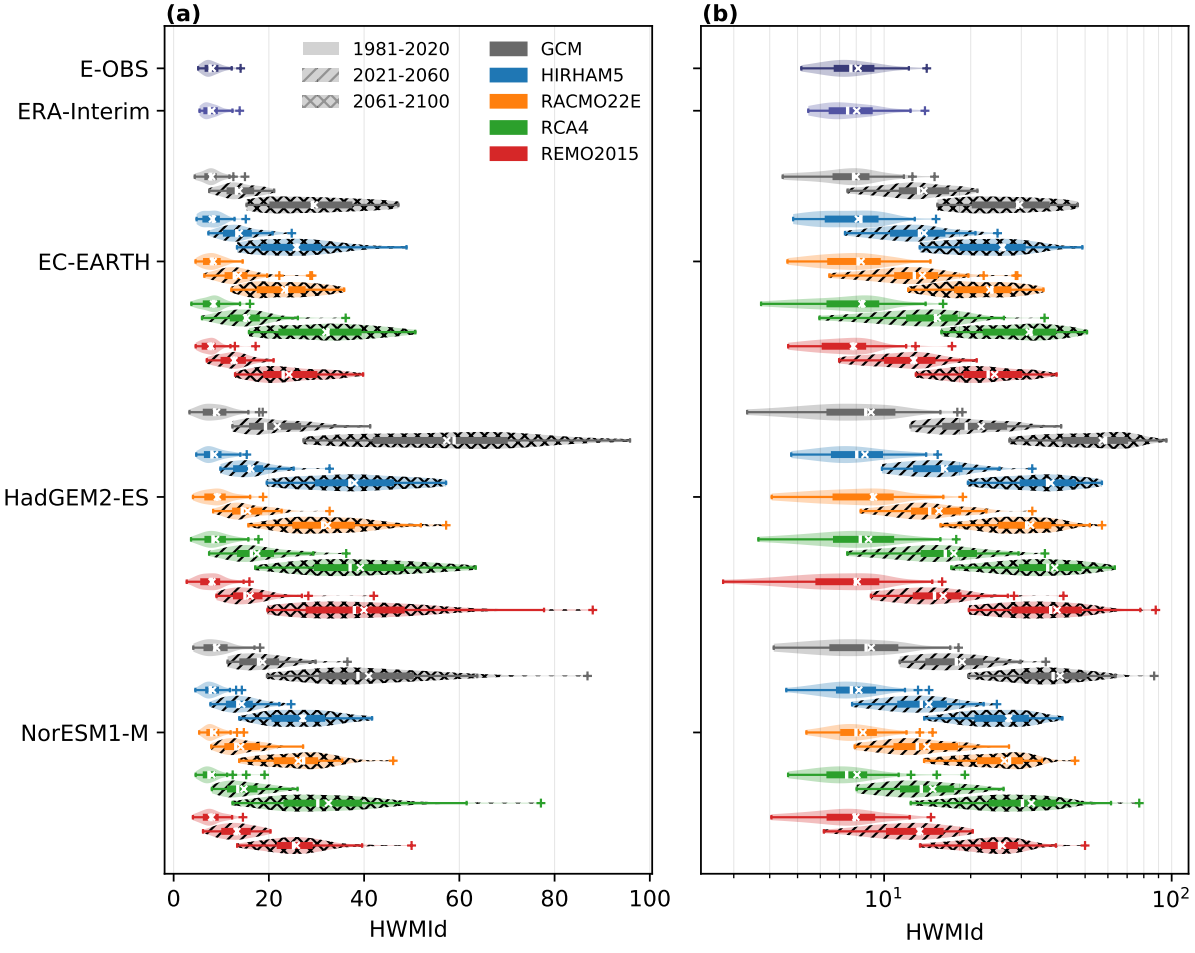

Figure 10. Violin/box plot for regional mean HWMId values under the defined three periods (indicated by filling patterns) in the simulation matrix of RCMs as well as the driving GCM simulations. Data are presented on different scales: (a) linear, and (b) logarithmic. Within each group (with one GCM), RCMs are identified by colors. Data from E-OBS and ERA-Interim are also shown for comparison under the recent past climate.

RCMs when driven by a same GCM generally share higher similarity with each other than with the driving GCM (Table S2), implicating a coherence for RCMs in representing heat wave magnitudes when downscaling GCMs.

Some scientists within the climate science community (e.g., Schiermeier, 2010; Kerr, 2011) show that uncertainty may increase when downscaling GCMs with RCMs as biases from the GCMs are conveyed to the RCMs and RCMs additionally add their own biases, referred to as the 'cascade of uncertainty' (e.g., Wilby and Dessai, 2010). However, many other studies (e.g., Torma et al., 2015; Di Luca et al., 2016; Rummukainen, 2016; Sørland et al., 2018; Strandberg and Lind, 2021) indicate that RCMs can also add value upon the driving GCM simulations. This study shows added value for heat wave magnitudes that have so far not been studied as extensively as for other aspects of climate and climate change. Such added value confirms

https://doi.org/10.5194/egusphere-2022-215
Preprint. Discussion started: 20 April 2022

the usefulness of RCMs for downscaling coarse-scale GCM simulations. Our analysis of the ensemble spread along the GCM dimension, reflecting uncertainty associated with driving data, reveals that the RCMs alter the spatial HWMId pattern from their driving GCM simulations, and that the alteration is different between the RCMs (Fig. 5 and Table S3). This suggests that the uncertainties of GCMs in simulating heat wave magnitudes would be transformed by RCMs, rather than simply inherited, due to the nonlinear nature of model dynamics and physics.

To reveal the specific factors/processes behind the added value of RCMs in simulating heat wave magnitudes, however, further analysis is required. Table 4 and Fig. 3, show clearly that RCMs capture the HWMId better than the GCMs for the recent past. An interesting finding of this study is that some spatial features of HWMId related to orographic effects can be seen as one aspect of the added value of RCMs; nevertheless, orographic effects are differently represented across the RCMs, suggesting that the representation of orographic effects is one of the major sources of uncertainty. This supports the statement by Sørland et al. (2018) that increasing the spatial resolution should not be the single factor contributing to the added value of RCMs.

4.2 Possible processes behind the climate change signals

The RCMs, as well as the driving GCMs, project a rise in HWMId values at an exponential-like rate under RCP8.5 on the European continent. As a result, heat waves more severe than the most severe one that has been experienced until now are projected to occur almost every year at the end of the century. According to the definition of HMWId, the exponential-like rise can be expected because the projected warming will on one hand increase the daily magnitude (Eq. 2) and on the other hand, with a strong probability, extend the duration simultaneously. Apart from the agreement on the alarm on the future severity of heat waves under this scenario, the RCMs modify the future climate change signals projected by the driving GCMs, tending to moderate the rise in HWMId values and also deliver some different features in the spatial pattern. The underlying drivers of heat waves may be related to land-atmosphere interactions as well as atmospheric processes (Horton et al., 2016; Liu et al., 2020). Understanding how RCMs differ from GCMs in representing processes that modify the climate change signals can have implications for how to utilize model projections in studies on climate change mitigation and adaptation.

Rather than directly investigating the associated processes, we investigate the corresponding climate change signals in annual mean $T_{\max}$ (Fig. S1), dry days (Fig. S2), and effective precipitation (Fig. S3). According to the definition of HWMId, the surge in heat wave magnitude is expected from the projected warming implying that a strong increase in $T_{\max}$ is expected. An increase of the annual number of dry days may indicate a higher tendency of longer warm spells and hence a rise in HWMId. Compared to the number of dry days, effective precipitation is more strongly related to dry soil conditions; the correlation between effective precipitation and HWMId may reveal the effect of land-atmosphere feedbacks, as the deficit in soil moisture may reduce latent heat flux allowing temperatures to rise further (Zhang et al., 2020).

The RCMs dampen the increase, and to some extent modify the spatial pattern, in the annual mean of daily maximum temperature in HadGEM2-ES and NorESM1-M (Fig. S1 and Table S4). This could potentially explain the more moderate rise in HWMId simulated by the RCMs compared to their driving GCMs. EC-EARTH and its downscaling by the RCMs show a similar level of increase as well as a similar spatial pattern in the annual mean of maximum temperature (Fig. S1

https://doi.org/10.5194/egusphere-2022-215
Preprint. Discussion started: 20 April 2022

and Table S4), and we recognize that they also project a similar rise in HWMId (Fig. 6). For the annual number of dry days (Fig. S2), on regional average, the RCMs also reduce the increase from their driving GCMs, but with a few exceptions (e.g., HIRHAM5 downloading EC-EARTH and HadGEM2-ES). For annual effective precipitation (Fig. S3), on a continental basis, the RCMs, except for HIRHAM5, show a smaller decrease (or larger increase) than the driving GCMs. In general, these results are consistent with Coppola et al. (2021) who discussed similar indices.

The results implicate that processes relating to land-atmosphere feedbacks may also play a role. By examining the spatial correlation between the change in HWMId and that in the three indices, we attempt to explore how these processes modulate the climate change signals in HWMId. The case becomes complicated when it comes to local features and it is not evident how annual mean statistics may influence individual heat waves and thereby the HWMId. Taking the change signals in annual effective precipitation as an example, compared to the driving GCMs, the RCMs tend to amplify both the decrease in the south and the increase in the north but exhibit a smaller decrease on a continental basis. For the detailed spatial pattern of the change in HWMId, it cannot be explained by the change in the annual mean of daily maximum temperature alone, even though HWMId is calculated based only on daily maximum temperature. The drying trend in southern Europe simulated by the models seems to contribute to the rise in HWMId, while the wetting trend in northern Europe may moderate the rise in HWMId in that region. We also observe a poor spatial correlation between the change in HWMId and that in the annual mean of daily maximum temperature for the GCM simulations (Fig. S1), which implies that the spatial pattern of the change in HWMId simulated by the GCMs is regulated rather by the durations of heat waves than by the magnitudes of daily maximum temperature. Indeed, the change in HWMId has a relatively close correlation with the change in the annual number of dry days for the GCMs (except for HadGEM2-ES at 2021-2060), with spatial r values around 0.5, which are also higher than those for all the RCMs other than REMO2015 (Fig. S2). This pattern is even more apparent for annual effective precipitation (Fig. S3). For the RCMs, it seems that the general warming together with other processes (e.g., relating to land-atmosphere feedbacks) regulates the spatial pattern of the rise in HWMId. Further studies detailed on the projected climate change signals in large-scale circulations (e.g., atmospheric blocking) and land surface fluxes are expected to reveal more information about the possible processes behind the climate change signals in heat wave magnitudes.

5 Summary and conclusions

By deploying the HWMId index, the study addresses how four different RCMs downscaling i) reanalysis and ii) three different GCMs, represent European heat wave magnitudes.

Initially, the performance of the RCMs in reproducing historical heat wave magnitudes is evaluated by comparing the ERA-Interim-driven evaluation runs of the RCMs with observational data. It shows that the RCMs generally capture most spatial and temporal features of the observed HWMId, suggesting the RCMs as a reliable tool for simulating heat wave magnitudes but still with room for improvement. Our results endorse the added value of RCMs over GCMs in representing the observed heat wave magnitudes. Compared to the driving GCMs the RCMs generally have lower RMSE and higher r against the observational data for the climatological mean of HWMId values under the recent past climate. In general, the RCMs improve spatial pattern

https://doi.org/10.5194/egusphere-2022-215
Preprint. Discussion started: 20 April 2022

of HWMId across the European continent compared to the driving GCMs. In addition, the RCMs reveal some small-scale features (e.g., relating to orographic effects) that the GCMs fail likely due to their coarse resolutions. The closest agreement with observations is seen for the RCM ensemble mean.

A rise in HWMId at an exponential-like rate is projected consistently by all the GCM and RCM simulations accounted for in the study, probably because the warming boosts both the intensity and duration. However, the RCMs modify some feature of the climate change signals in the driving GCM simulations. A relatively more moderate rising rate across the European continent is projected by the RCMs, as a corresponding result of the reduced warming. The weaker drying trend in the RCMs may also contribute to the weaker climate change signals in heat wave magnitudes. The RCMs also differ from the driving GCMs in the spatial pattern of the climate change signals of HWMId. All the GCM and RCM simulations agree on the stronger increase in HWMId in southern Europe, which is very likely amplified by the projected drying trend. As a direct consequence of more rapid warming in northern Europe an expected higher HWMId increase in this region is seen in the RCM simulations only. By this token, the general warming play a small role in regulating the spatial pattern of the change in HWMId in GCM simulations, different from the case of the RCMs.

We also analyzed the uncertainties of the RCM simulation matrix in simulating heat wave magnitudes. The results show that the uncertainty associated with choice of RCM is of similar importance as with driving data. The ensemble spread/mean ratio is approximately one fifth for the present-climate HWMId, and becomes over half for the climate change signals. A major source of the uncertainty associated with the RCMs appears to be associated with the representation of orographic effects. The RCMs reduce the large ensemble spread across the GCM simulations though, especially for the climate change signals in HWMId. Moreover, no consistent spatial pattern is observed in the ensemble spreads along the GCM dimension for different RCMs. Consequently, the results indicate that the uncertainties of GCMs in simulating heat wave magnitudes would not be simply inherited by RCMs but are transformed in a complex manner due to the nonlinear nature of model dynamics and physics.

Code availability. All the analyses were done using Python packages.

Data availability. The EURO-CORDEX RCM data and the CMIP5 GCM data analyzed in this work are available for download via the Earth System Grid Federation (ESGF) under the project name “CORDEX” and “CMIP5”, respectively, at the NSC-LIU-SMHI (Swedish) datanode: https://esg-dn1.nsc.liu.se/projects/esgf-liu/ (last access: April 14, 2022). The E-OBS data are available for download via the ECA&D project: https://www.ecad.eu/ (last access: April 14, 2022). The ERA-Interim reanalysis data from ECMWF can be accessed using their Meteorological Archival and Retrieval System (MARS): https://www.ecmwf.int/en/forecasts/datasets/reanalysis-datasets/era-interim (last access: April 14, 2022).

Author contributions. CL set up the analysis framework with the scientific contributions of EK and RW. CL produced the figures and tables. CL wrote the publication with important contributions from EK, RW and DC.

https://doi.org/10.5194/egusphere-2022-215
Preprint. Discussion started: 20 April 2022

Competing interests. The contact author has declared that neither they nor their co-authors have any competing interests.

Acknowledgements. This work is partly supported by Swedish FORMAS (2018-02858 and 2019-01520) and VR (2019-03954). The authors would like to thank the EURO-CORDEX network (https://www.euro-cordex.net/) and WCRP CORDEX (https://cordex.org/) for ensuring availability of CORDEX data. We acknowledge the E-OBS dataset from the EU-FP6 project UERRA (https://www.uerra.eu/) and the Copernicus Climate Change Service, and the data providers in the ECA&D project (https://www.ecad.eu/).

https://doi.org/10.5194/egusphere-2022-215
Preprint. Discussion started: 20 April 2022

References

Åström, C., Bjelkmar, P., and Forsberg, B.: Attributing summer mortality to heat during 2018 heatwave in Sweden, Environmental Epidemiology, 3, 16–17, https://doi.org/10.1097/01.EE9.0000605788.56297.b5, 2019.

Barriopedro, D., Fischer, E. M., Luterbacher, J., Trigo, R. M., and García-Herrera, R.: The hot summer of 2010: redrawing the temperature record map of Europe, Science, 332, 220–224, https://doi.org/10.1126/science.1201224, 2011.

Ceccherini, G., Russo, S., Ameztoy, I., Marchese, A. F., and Carmona-Moreno, C.: Heat waves in Africa 1981–2015, observations and reanalysis, Natural Hazards and Earth System Sciences, 17, 115–125, https://doi.org/10.5194/nhess-17-115-2017, 2017.

Coppola, E., Nogherotto, R., Ciarlò, J. M., Giorgi, F., van Meijgaard, E., Kadygrov, N., Iles, C., Corre, L., Sandstad, M., Somot, S., Nabat, P., Vautard, R., Levavasseur, G., Schwingshackl, C., Sillmann, J., Kjellström, E., Nikulin, G., Aalbers, E., Lenderink, G., Christensen, O. B., Boberg, F., Sørland, S. L., Demory, M.-E., Bülow, K., Teichmann, C., Warrach-Sagi, K., and Wulfmeyer, V.: Assessment of the European Climate Projections as Simulated by the Large EURO-CORDEX Regional and Global Climate Model Ensemble, Journal of Geophysical Research: Atmospheres, 126, e2019JD032 356, https://doi.org/10.1029/2019JD032356, 2021.

Cornes, R. C., van der Schrier, G., van den Besselaar, E. J. M., and Jones, P. D.: An Ensemble Version of the E-OBS Temperature and Precipitation Data Sets, Journal of Geophysical Research: Atmospheres, 123, 9391–9409, https://doi.org/10.1029/2017JD028200, 2018.

Dee, D. P., Uppala, S. M., Simmons, A., Berrisford, P., Poli, P., Kobayashi, S., Andrae, U., Balmaseda, M., Balsamo, G., Bauer, d. P., et al.: The ERA-Interim reanalysis: Configuration and performance of the data assimilation system, Quarterly Journal of the royal meteorological society, 137, 553–597, https://doi.org/10.1002/qj.828, 2011.

Di Luca, A., Argüeso, D., Evans, J. P., de Elía, R., and Laprise, R.: Quantifying the overall added value of dynamical downscaling and the contribution from different spatial scales, Journal of Geophysical Research: Atmospheres, 121, 1575–1590, https://doi.org/10.1002/2015JD024009, 2016.

Dosio, A., Mentaschi, L., Fischer, E. M., and Wyser, K.: Extreme heat waves under 1.5 °C and 2 °C global warming, Environmental Research Letters, 13, 054 006, https://doi.org/10.1088/1748-9326/aab827, 2018.

Eyring, V., Bony, S., Meehl, G. A., Senior, C. A., Stevens, B., Stouffer, R. J., and Taylor, K. E.: Overview of the Coupled Model Intercomparison Project Phase 6 (CMIP6) experimental design and organization, Geoscientific Model Development, 9, 1937–1958, https://doi.org/10.5194/gmd-9-1937-2016, 2016.

Giorgi, F., Jones, C., and Asrar, G. R.: Addressing climate information needs at the regional level: the CORDEX framework, World Meteorological Organization (WMO) Bulletin, 58, 175, 2009.

Guo, Y., Gasparrini, A., Armstrong, B. G., Tawatsupa, B., Tobias, A., Lavigne, E., de Sousa Zanotti Stagliorio Coelho, M., Pan, X., Kim, H., Hashizume, M., Honda, Y., Guo, Y.-L. L., Wu, C.-F., Zanobetti, A., Schwartz, J. D., Bell, M. L., Scortichini, M., Michelozzi, P., Punnasiri, K., Li, S., Tian, L., Garcia, S. D. O., Seposo, X., Overcenco, A., Zeka, A., Goodman, P., Dang, T. N., Dung, D. V., Mayvaneh, F., Saldiva, P. H. N., Williams, G., and Tong, S.: Heat wave and mortality: a multicountry, multicommunity study, Environmental health perspectives, 125, 087 006, https://doi.org/10.1289/EHP1026, 2017.

Horton, R. M., Mankin, J. S., Lesk, C., Coffel, E., and Raymond, C.: A review of recent advances in research on extreme heat events, Current Climate Change Reports, 2, 242–259, https://doi.org/10.1007/s40641-016-0042-x, 2016.

IPCC: Part A: Global and Sectoral Aspects, in: Climate Change 2014: Impacts, Adaptation, and Vulnerability. Working Group II Contribution to the Fifth Assessment Report of the Intergovernmental Panel on Climate Change, edited by Field, C., Van Aalst, M., Aalst, M., Adger, W., Arent, D., Barnett, J., Betts, R., Bilir, E., Birkmann, J., Carmin, J., Chadee, D., Challinor, A., Chatterjee, M., Cramer, W., Davidson,

https://doi.org/10.5194/egusphere-2022-215
Preprint. Discussion started: 20 April 2022

D., Estrada, Y., Gattuso, J.-P., Hijioka, Y., Guldberg, O., Huang, H.-Q., Insarov, G., Jones, R., Kovats, S., Lankao, P., Larsen, J., nigo Losada, I., Marengo, J., McLean, R., Mearns, L., Mechler, R., Morton, J., Niang, I., Oki, T., Olwoch, J., Opondo, M., Poloczanska, E., Pörtner, H.-O., Redsteer, M., Reisinger, A., Revi, A., Schmidt, D., Shaw, R., Solecki, W., Stone, D., Stone, J., Strzepek, K., Suarez, A., Tschakert, P., Valentini, R., Vicuna, S., Villamizar, A., Vincent, K., Warren, R., White, L., Wilbanks, T., Wong, P., and Yoh, G., p. 1132, Cambridge University Press, Cambridge, United Kingdom and New York, NY, USA, 2014.

IPCC: Summary for Policymakers, in: Global Warming of 1.5°C. An IPCC Special Report on the impacts of global warming of 1.5°C above pre-industrial levels and related global greenhouse gas emission pathways, in the context of strengthening the global response to the threat of climate change, sustainable development, and efforts to eradicate poverty, edited by Masson-Delmotte, V., Zhai, P., Pörtner, H.-O., Roberts, D., Skea, J., Shukla, P., Pirani, A., Moufouma-Okia, W., Péan, C., Pidcock, R., Connors, S., Matthews, J., Chen, Y., Zhou, X., Gomis, M., Lonnoy, E., Maycock, T., Tignor, M., and Waterfield, T., p. 32, World Meteorological Organization, Geneva, Switzerland, 2018.

IPCC: Summary for Policymakers, in: Climate Change 2022: Impacts, Adaptation, and Vulnerability. Working Group II Contribution to the Sixth Assessment Report of the Intergovernmental Panel on Climate Change, edited by Pörtner, H.-O., Roberts, D., Poloczanska, E., Mintenbeck, K., Tignor, M., Alegría, A., Craig, M., Langsdorf, S., Löschke, S., Möller, V., and Okem, A., p. 37, Cambridge University Press, Cambridge, United Kingdom and New York, NY, USA, in Press, 2022.

Jacob, D., Bärring, L., Christensen, O. B., Christensen, J. H., de Castro, M., Deque, M., Giorgi, F., Hagemann, S., Hirschi, M., Jones, R., et al.: An inter-comparison of regional climate models for Europe: model performance in present-day climate, Climatic change, 81, 31–52, https://doi.org/10007/s10584-006-9213-4, 2007.

Jacob, D., Teichmann, C., Sobolowski, S., Katragkou, E., Anders, I., Belda, M., Benestad, R., Boberg, F., Buonomo, E., Cardoso, R. M., Casanueva, A., Christensen, O. B., Christensen, J. H., Coppola, E., Cruz, L. D., Davin, E. L., Dobler, A., Domínguez, M., Fealy, R., Fernandez, J., Gaertner, M. A., García-Díez, M., Giorgi, F., Gobiet, A., Goergen, K., Gómez-Navarro, J. J., Alemán, J. J. G., Gutiérrez, C., Gutiérrez, J. M., Güttler, I., Haensler, A., Halenka, T., Jerez, S., Jiménez-Guerrero, P., Jones, R. G., Keuler, K., Kjellström, E., Knist, S., Kotlarski, S., Maraun, D., van Meijgaard, E., Mercogliano, P., Montávez, J. P., Navarra, A., Nikulin, G., de Noblet-Ducoudré, N., Panitz, H.-J., Pfeifer, S., Piazza, M., Pichelli, E., Pietikäinen, J.-P., Prein, A. F., Preuschmann, S., Rechid, D., Rockel, B., Romera, R., Sánchez, E., Sieck, K., Soares, P. M. M., Somot, S., Srnec, L., Sørland, S. L., Termonia, P., Truhetz, H., Vautard, R., Warrach-Sagi, K., and Wulfmeyer, V.: Regional climate downscaling over Europe: perspectives from the EURO-CORDEX community, Regional environmental change, 20, 1–20, https://doi.org/10.1007/s10113-020-01606-9, 2020.

Jerez, S., Palacios-Peña, L., Gutiérrez, C., Jiménez-Guerrero, P., López-Romero, J. M., Pravia-Sarabia, E., and Montávez, J. P.: Sensitivity of surface solar radiation to aerosol–radiation and aerosol–cloud interactions over Europe in WRFv3. 6.1 climatic runs with fully interactive aerosols, Geoscientific Model Development, 14, 1533–1551, https://doi.org/10.5194/gmd-14-1533-2021, 2021.

Kerr, R. A.: Vital Details of Global Warming Are Eluding Forecasters, Science, 334, 173–174, https://doi.org/10.1126/science.334.6053.173, 2011.

Liu, X., He, B., Guo, L., Huang, L., and Chen, D.: Similarities and differences in the mechanisms causing the European summer heatwaves in 2003, 2010, and 2018, Earth's Future, 8, e2019EF001 386, https://doi.org/10.1029/2019EF001386, 2020.

Luo, Z., Yang, J., Gao, M., and Chen, D.: Extreme hot days over three global mega-regions: Historical fidelity and future projection, Atmospheric Science Letters, 21, e1003, https://doi.org/10.1002/asl.1003, 2020.

Molina, M., Sánchez, E., and Gutiérrez, C.: Future heat waves over the Mediterranean from an Euro-CORDEX regional climate model ensemble, Scientific Reports, 10, 1–10, https://doi.org/10.1038/s41598-020-65663-0, 2020.

https://doi.org/10.5194/egusphere-2022-215
Preprint. Discussion started: 20 April 2022

Perkins, S. E. and Alexander, L. V.: On the measurement of heat waves, Journal of Climate, 26, 4500–4517, https://doi.org/10.1175/JCLI-D-12-00383.1, 2013.

Rennie, S., Goergen, K., Wohner, C., Apweiler, S., Peterseil, J., and Watkins, J.: A climate service for ecologists: sharing pre-processed EURO-CORDEX regional climate scenario data using the eLTER Information System, Earth System Science Data, 13, 631–644, https://doi.org/10.5194/essd-13-631-2021, 2021.

Robine, J.-M., Cheung, S. L. K., Le Roy, S., Van Oyen, H., Griffiths, C., Michel, J.-P., and Herrmann, F. R.: Death toll exceeded 70,000 in Europe during the summer of 2003, Comptes rendus biologies, 331, 171–178, https://doi.org/10.1016/j.crvi.2007.12.001, 2008.

Rummukainen, M.: Added value in regional climate modeling, Wiley Interdisciplinary Reviews: Climate Change, 7, 145–159, https://doi.org/10.1002/wcc.378, 2016.

Russo, S., Sillmann, J., and Fischer, E. M.: Top ten European heatwaves since 1950 and their occurrence in the coming decades, Environmental Research Letters, 10, 124 003, https://doi.org/10.1088/1748-9326, 2015.

Russo, S., Marchese, A. F., Sillmann, J., and Immé, G.: When will unusual heat waves become normal in a warming Africa?, Environmental Research Letters, 11, 054 016, https://doi.org/10.1088/1748-9326/11/5/054016, 2016.

Schiermeier, Q.: The real holes in climate science: like any other field, research on climate change has some fundamental gaps, although not the ones typically claimed by sceptics. Quirin Schiermeier takes a hard look at some of the biggest problem areas, Nature, 463, 284–288, https://doi.org/10.1038/463284a, 2010.

Seneviratne, S. I., Zhang, X., Adnan, M., Badi, W., Dereczynski, C., Di Luca, A., Ghosh, S., Iskandar, I., Kossin, J., Lewis, S., Otto, F., Pinto, I., Satoh, M., Vicente-Serrano, S. M., Wehner, M., and Zhou, B.: Weather and climate extreme events in a changing climate, in: Climate change 2021: the physical science basis. Contribution of Working Group I to the Sixth Assessment Report of the Intergovernmental Panel on Climate Change, edited by Masson-Delmotte, V., Zhai, P., Pirani, A., Connors, S. L., Péan, C., Berger, S., Caud, N., Chen, Y., Goldfarb, L., Gomis, M. I., Huang, M., Leitzell, K., Lonnoy, E., Matthews, J. B. R., Maycock, T. K., Waterfield, T., Yelekçi, O., Yu, R., and Zhou, B., p. 345, Cambridge University Press, Cambridge, United Kingdom and New York, NY, USA, 2021.

Sørland, S. L., Schär, C., Lüthi, D., and Kjellström, E.: Bias patterns and climate change signals in GCM-RCM model chains, Environmental Research Letters, 13, 074 017, https://doi.org/10.1088/1748-9326/aacc77, 2018.

Sørland, S. L., Fischer, A. M., Kotlarski, S., Künsch, H. R., Liniger, M. A., Rajczak, J., Schär, C., Spirig, C., Strassmann, K., and Knutti, R.: CH2018–National climate scenarios for Switzerland: How to construct consistent multi-model projections from ensembles of opportunity, Climate Services, 20, 100 196, https://doi.org/10.1016/j.cliser.2020.100196, 2020.

Strandberg, G. and Lind, P.: The importance of horizontal model resolution on simulated precipitation in Europe–from global to regional models, Weather and Climate Dynamics, 2, 181–204, https://doi.org/10.5194/wcd-2-181-2021, 2021.

Taylor, K. E., Stouffer, R. J., and Meehl, G. A.: An overview of CMIP5 and the experiment design, Bulletin of the American meteorological Society, 93, 485–498, https://doi.org/10.1175/BAMS-D-11-00094.1, 2012.

Torma, C., Giorgi, F., and Coppola, E.: Added value of regional climate modeling over areas characterized by complex terrain—Precipitation over the Alps, Journal of Geophysical Research: Atmospheres, 120, 3957–3972, https://doi.org/10.1002/2014JD022781, 2015.

Vautard, R., Kadygrov, N., Iles, C., Boberg, F., Buonomo, E., Bülow, K., Coppola, E., Corre, L., van Meijgaard, E., Nogherotto, R., Sandstad, M., Schwingshackl, C., Somot, S., Aalbers, E., Christensen, O. B., Ciarlò, J. M., Demory, M.-E., Giorgi, F., Jacob, D., Jones, R. G., Keuler, K., Kjellström, E., Lenderink, G., Levavasseur, G., Nikulin, G., Sillmann, J., Solidoro, C., Sørland, S. L., Steger, C., Teichmann, C., Warrach-Sagi, K., and Wulfmeyer, V.: Evaluation of the large EURO-CORDEX regional climate model ensemble, Journal of Geophysical Research: Atmospheres, n/a, e2019JD032 344, https://doi.org/10.1029/2019JD032344, 2020.

https://doi.org/10.5194/egusphere-2022-215
Preprint. Discussion started: 20 April 2022

Wilby, R. L. and Dessai, S.: Robust adaptation to climate change, Weather, 65, 180–185, https://doi.org/10.1002/wea.543, 2010.

Wilcke, R. A. I., Kjellström, E., Lin, C., Matei, D., Moberg, A., and Tyrlis, E.: The extremely warm summer of 2018 in Sweden–set in a historical context, Earth System Dynamics, 11, 1107–1121, https://doi.org/10.5194/esd-11-1107-2020, 2020.

Zampieri, M., Russo, S., di Sabatino, S., Michetti, M., Scoccimarro, E., and Gualdi, S.: Global assessment of heat wave magnitudes from 1901 to 2010 and implications for the river discharge of the Alps, Science of the Total Environment, 571, 1330–1339, https://doi.org/10.1016/j.scitotenv.2016.07.008, 2016.

Zhang, P., Jeong, J.-H., Yoon, J.-H., Kim, H., Wang, S.-Y. S., Linderholm, H. W., Fang, K., Wu, X., and Chen, D.: Abrupt shift to hotter and drier climate over inner East Asia beyond the tipping point, Science, 370, 1095–1099, https://doi.org/10.1126/science.abb3368, 2020.